

Observation of the decay $X(3872) \rightarrow \pi^0 \chi_{c1}(1P)$

M. Ablikim¹, M. N. Achasov^{10,d}, S. Ahmed¹⁵, M. Albrecht⁴, M. Alekseev^{55A,55C}, A. Amoroso^{55A,55C}, F. F. An¹, Q. An^{52,42}, Y. Bai⁴¹, O. Bakina²⁷, R. Baldini Ferroli^{23A}, Y. Ban³⁵, K. Begzsuren²⁵, J. V. Bennett⁵, N. Berger²⁶, M. Bertani^{23A}, D. Bettoni^{24A}, F. Bianchi^{55A,55C}, J. Bloms⁵⁰, I. Boyko²⁷, R. A. Briere⁵, H. Cai⁵⁷, X. Cai^{1,42}, A. Calcaterra^{23A}, G. F. Cao^{1,46}, N. Cao^{1,46}, S. A. Cetin^{45B}, J. Chai^{55C}, J. F. Chang^{1,42}, W. L. Chang^{1,46}, G. Chelkov^{27,b,c}, D. Y. Chen⁶, G. Chen¹, H. S. Chen^{1,46}, J. C. Chen¹, M. L. Chen^{1,42}, S. J. Chen³³, Y. B. Chen^{1,42}, W. Cheng^{55C}, G. Cibinetto^{24A}, F. Cossio^{55C}, X. F. Cui³⁴, H. L. Dai^{1,42}, J. P. Dai^{37,h}, X. C. Dai^{1,46}, A. Dbeyssi¹⁵, D. Dedovich²⁷, Z. Y. Deng¹, A. Denig²⁶, I. Denysenko²⁷, M. Destefanis^{55A,55C}, F. De Mori^{55A,55C}, Y. Ding³¹, C. Dong³⁴, J. Dong^{1,42}, L. Y. Dong^{1,46}, M. Y. Dong^{1,42,46}, Z. L. Dou³³, S. X. Du⁶⁰, J. Z. Fan⁴⁴, J. Fang^{1,42}, S. S. Fang^{1,46}, Y. Fang¹, R. Farinelli^{24A,24B}, L. Fava^{55B,55C}, F. Feldbauer⁴, G. Felici^{23A}, C. Q. Feng^{52,42}, M. Fritsch⁴, C. D. Fu¹, Y. Fu¹, Q. Gao¹, X. L. Gao^{52,42}, Y. Gao⁵³, Y. Gao⁴⁴, Y. G. Gao⁶, Z. Gao^{52,42}, B. Garillon²⁶, I. Garzia^{24A}, A. Gilman⁴⁹, K. Goetzen¹¹, L. Gong³⁴, W. X. Gong^{1,42}, W. Gradl²⁶, M. Greco^{55A,55C}, L. M. Gu³³, M. H. Gu^{1,42}, S. Gu², Y. T. Gu¹³, A. Q. Guo²², L. B. Guo³², R. P. Guo^{1,46}, Y. P. Guo²⁶, A. Guskov²⁷, S. Han⁵⁷, X. Q. Hao¹⁶, F. A. Harris⁴⁷, K. L. He^{1,46}, F. H. Heinsius⁴, T. Held⁴, Y. K. Heng^{1,42,46}, Y. R. Hou⁴⁶, Z. L. Hou¹, H. M. Hu^{1,46}, J. F. Hu^{37,h}, T. Hu^{1,42,46}, Y. Hu¹, G. S. Huang^{52,42}, J. S. Huang¹⁶, X. T. Huang³⁶, X. Z. Huang³³, N. Huesken⁵⁰, T. Hussain⁵⁴, W. Ikegami Andersson⁵⁶, W. Imoehl²², M. Irshad^{52,42}, Q. Ji¹, Q. P. Ji¹⁶, X. B. Ji^{1,46}, X. L. Ji^{1,42}, H. L. Jiang³⁶, X. S. Jiang^{1,42,46}, X. Y. Jiang³⁴, J. B. Jiao³⁶, Z. Jiao¹⁸, D. P. Jin^{1,42,46}, S. Jin³³, Y. Jin⁴⁸, T. Johansson⁵⁶, N. Kalantar-Nayestanaki²⁹, X. S. Kang³¹, R. Kappert²⁹, M. Kavatsyuk²⁹, B. C. Ke¹, I. K. Keshk⁴, T. Khan^{52,42}, A. Khoukaz⁵⁰, P. Kiese²⁶, R. Kiuchi¹, R. Kliemt¹¹, L. Koch²⁸, O. B. Kolcu^{45B,f}, B. Kopf⁴, M. Kuemmel⁴, M. Kuessner⁴, A. Kupsc⁵⁶, M. Kurth¹, M. G. Kurth^{1,46}, W. Kühn²⁸, J. S. Lange²⁸, P. Larin¹⁵, L. Lavezzi^{55C}, H. Leithoff²⁶, T. Lenz²⁶, C. Li⁵⁶, Cheng Li^{52,42}, D. M. Li⁶⁰, F. Li^{1,42}, F. Y. Li³⁵, G. Li¹, H. B. Li^{1,46}, H. J. Li^{9,j}, J. C. Li¹, J. W. Li⁴⁰, Ke Li¹, L. K. Li¹, Lei Li³, P. L. Li^{52,42}, P. R. Li³⁰, Q. Y. Li³⁶, W. D. Li^{1,46}, W. G. Li¹, X. H. Li^{52,42}, X. L. Li³⁶, X. N. Li^{1,42}, X. Q. Li³⁴, Z. B. Li⁴³, H. Liang^{1,46}, H. Liang^{52,42}, Y. F. Liang³⁹, Y. T. Liang²⁸, G. R. Liao¹², L. Z. Liao^{1,46}, J. Libby²¹, C. X. Lin⁴³, D. X. Lin¹⁵, Y. J. Lin¹³, B. Liu^{37,h}, B. J. Liu¹, C. X. Liu¹, D. Liu^{52,42}, D. Y. Liu^{37,h}, F. H. Liu³⁸, Fang Liu¹, Feng Liu⁶, H. B. Liu¹³, H. M. Liu^{1,46}, Huanhuan Liu¹, Huihui Liu¹⁷, J. B. Liu^{52,42}, J. Y. Liu^{1,46}, K. Y. Liu³¹, Ke Liu⁶, Q. Liu⁴⁶, S. B. Liu^{52,42}, T. Liu^{1,46}, X. Liu³⁰, X. Y. Liu^{1,46}, Y. B. Liu³⁴, Z. A. Liu^{1,42,46}, Zhiqing Liu²⁶, Y. F. Long³⁵, X. C. Lou^{1,42,46}, H. J. Lu¹⁸, J. D. Lu^{1,46}, J. G. Lu^{1,42}, Y. Lu¹, Y. P. Lu^{1,42}, C. L. Luo³², M. X. Luo⁵⁹, P. W. Luo⁴³, T. Luo^{9,j}, X. L. Luo^{1,42}, S. Lusso^{55C}, X. R. Lyu⁴⁶, F. C. Ma³¹, H. L. Ma¹, L. L. Ma³⁶, M. M. Ma^{1,46}, Q. M. Ma¹, X. N. Ma³⁴, X. X. Ma^{1,46}, X. Y. Ma^{1,42}, Y. M. Ma³⁶, F. E. Maas¹⁵, M. Maggiora^{55A,55C}, S. Maldaner²⁶, Q. A. Malik⁵⁴, A. Mangoni^{23B}, Y. J. Mao³⁵, Z. P. Mao¹, S. Marcello^{55A,55C}, Z. X. Meng⁴⁸, J. G. Messchendorp²⁹, G. Mezzadri^{24A}, J. Min^{1,42}, T. J. Min³³, R. E. Mitchell²², X. H. Mo^{1,42,46}, Y. J. Mo⁶, C. Morales Morales¹⁵, N. Yu. Muchnoi^{10,d}, H. Muramatsu⁴⁹, A. Mustafa⁴, S. Nakhoul^{11,g}, Y. Nefedov²⁷, F. Nerling^{11,g}, I. B. Nikolaev^{10,d}, Z. Ning^{1,42}, S. Nisar^{8,k}, S. L. Niu^{1,42}, S. L. Olsen⁴⁶, Q. Ouyang^{1,42,46}, S. Pacetti^{23B}, Y. Pan^{52,42}, M. Papenbrock⁵⁶, P. Patteri^{23A}, M. Pelizaeus⁴, H. P. Peng^{52,42}, K. Peters^{11,g}, J. Pettersson⁵⁶, J. L. Ping³², R. G. Ping^{1,46}, A. Pitka⁴, R. Poling⁴⁹, V. Prasad^{52,42}, M. Qi³³, T. Y. Qi², S. Qian^{1,42}, C. F. Qiao⁴⁶, N. Qin⁵⁷, X. P. Qin¹³, X. S. Qin⁴, Z. H. Qin^{1,42}, J. F. Qiu¹, S. Q. Qu³⁴, K. H. Rashid^{54,i}, C. F. Redmer²⁶, M. Richter⁴, M. Ripka²⁶, A. Rivetti^{55C}, M. Rolo^{55C}, G. Rong^{1,46}, Ch. Rosner¹⁵, M. Rump⁵⁰, A. Sarantsev^{27,e}, M. Savrié^{24B}, K. Schoenning⁵⁶, W. Shan¹⁹, X. Y. Shan^{52,42}, M. Shao^{52,42}, C. P. Shen², P. X. Shen³⁴, X. Y. Shen^{1,46}, H. Y. Sheng¹, X. Shi^{1,42}, X. D. Shi^{52,42}, J. J. Song³⁶, Q. Q. Song^{52,42}, X. Y. Song¹, S. Sosio^{55A,55C}, C. Sowa⁴, S. Spataro^{55A,55C}, F. F. Sui³⁶, G. X. Sun¹, J. F. Sun¹⁶, L. Sun⁵⁷, S. S. Sun^{1,46}, X. H. Sun¹, Y. J. Sun^{52,42}, Y. K. Sun^{52,42}, Y. Z. Sun¹, Z. J. Sun^{1,42}, Z. T. Sun¹, Y. T. Tan^{52,42}, C. J. Tang³⁹, G. Y. Tang¹, X. Tang¹, V. Thoren⁵⁶, B. Tsednee²⁵, I. Uman^{45D}, B. Wang¹, B. L. Wang⁴⁶, C. W. Wang³³, D. Y. Wang³⁵, H. H. Wang³⁶, K. Wang^{1,42}, L. L. Wang¹, L. S. Wang¹, M. Wang³⁶, M. Z. Wang³⁵, Meng Wang^{1,46}, P. Wang¹, P. L. Wang¹, R. M. Wang⁵⁸, W. P. Wang^{52,42}, X. Wang³⁵, X. F. Wang¹, Y. Wang^{52,42}, Y. F. Wang^{1,42,46}, Z. Wang^{1,42}, Z. G. Wang^{1,42}, Z. Y. Wang¹, Zongyuan Wang^{1,46}, T. Weber⁴, D. H. Wei¹², P. Weidenkaff²⁶, H. W. Wen³², S. P. Wen¹, U. Wiedner⁴, M. Wolke⁵⁶, L. H. Wu¹, L. J. Wu^{1,46}, Z. Wu^{1,42}, L. Xia^{52,42}, Y. Xia²⁰, S. Y. Xiao¹, Y. J. Xiao^{1,46}, Z. J. Xiao³², Y. G. Xie^{1,42}, Y. H. Xie⁶, T. Y. Xing^{1,46}, X. A. Xiong^{1,46}, Q. L. Xiu^{1,42}, G. F. Xu¹, J. J. Xu³³, L. Xu¹, Q. J. Xu¹⁴, W. Xu^{1,46}, X. P. Xu⁴⁰, F. Yan⁵³, L. Yan^{55A,55C}, W. B. Yan^{52,42}, W. C. Yan², Y. H. Yan²⁰, H. J. Yang^{37,h}, H. X. Yang¹, L. Yang⁵⁷, R. X. Yang^{52,42}, S. L. Yang^{1,46}, Y. H. Yang³³, Y. X. Yang¹², Yifan Yang^{1,46}, Z. Q. Yang²⁰, M. Ye^{1,42}, M. H. Ye⁷, J. H. Yin¹, Z. Y. You⁴³, B. X. Yu^{1,42,46}, C. X. Yu³⁴, J. S. Yu²⁰, C. Z. Yuan^{1,46}, X. Q. Yuan³⁵, Y. Yuan¹, A. Yuncu^{45B,a}, A. A. Zafar⁵⁴, Y. Zeng²⁰, B. X. Zhang¹, B. Y. Zhang^{1,42}, C. C. Zhang¹, D. H. Zhang¹, H. H. Zhang⁴³, H. Y. Zhang^{1,42}, J. Zhang^{1,46}, J. L. Zhang⁵⁸, J. Q. Zhang⁴, J. W. Zhang^{1,42,46}, J. Y. Zhang¹, J. Z. Zhang^{1,46},

K. Zhang^{1,46}, L. Zhang⁴⁴, S. F. Zhang³³, T. J. Zhang^{37,h}, X. Y. Zhang³⁶, Y. Zhang^{52,42}, Y. H. Zhang^{1,42},
 Y. T. Zhang^{52,42}, Yang Zhang¹, Yao Zhang¹, Yu Zhang⁴⁶, Z. H. Zhang⁶, Z. P. Zhang⁵², Z. Y. Zhang⁵⁷, G. Zhao¹,
 J. W. Zhao^{1,42}, J. Y. Zhao^{1,46}, J. Z. Zhao^{1,42}, Lei Zhao^{52,42}, Ling Zhao¹, M. G. Zhao³⁴, Q. Zhao¹, S. J. Zhao⁶⁰,
 T. C. Zhao¹, Y. B. Zhao^{1,42}, Z. G. Zhao^{52,42}, A. Zhemchugov^{27,b}, B. Zheng⁵³, J. P. Zheng^{1,46}, Y. Zheng³⁵,
 Y. H. Zheng⁴⁶, B. Zhong³², L. Zhou^{1,42}, L. P. Zhou^{1,46}, Q. Zhou^{1,46}, X. Zhou⁵⁷, X. K. Zhou⁴⁶, X. R. Zhou^{52,42},
 Xiaoyu Zhou²⁰, Xu Zhou²⁰, A. N. Zhu^{1,46}, J. Zhu³⁴, J. Zhu⁴³, K. Zhu¹, K. J. Zhu^{1,42,46}, S. H. Zhu⁵¹,
 W. J. Zhu³⁴, X. L. Zhu⁴⁴, Y. C. Zhu^{52,42}, Y. S. Zhu^{1,46}, Z. A. Zhu^{1,46}, J. Zhuang^{1,42}, B. S. Zou¹, J. H. Zou¹¹

(BESIII Collaboration)

¹ *Institute of High Energy Physics, Beijing 100049, People's Republic of China*

² *Beihang University, Beijing 100191, People's Republic of China*

³ *Beijing Institute of Petrochemical Technology, Beijing 102617, People's Republic of China*

⁴ *Bochum Ruhr-University, D-44780 Bochum, Germany*

⁵ *Carnegie Mellon University, Pittsburgh, Pennsylvania 15213, USA*

⁶ *Central China Normal University, Wuhan 430079, People's Republic of China*

⁷ *China Center of Advanced Science and Technology, Beijing 100190, People's Republic of China*

⁸ *COMSATS University Islamabad, Lahore Campus,*

Defence Road, Off Raiwind Road, 54000 Lahore, Pakistan

⁹ *Fudan University, Shanghai 200443, People's Republic of China*

¹⁰ *G.I. Budker Institute of Nuclear Physics SB RAS (BINP), Novosibirsk 630090, Russia*

¹¹ *GSI Helmholtzcentre for Heavy Ion Research GmbH, D-64291 Darmstadt, Germany*

¹² *Guangxi Normal University, Guilin 541004, People's Republic of China*

¹³ *Guangxi University, Nanning 530004, People's Republic of China*

¹⁴ *Hangzhou Normal University, Hangzhou 310036, People's Republic of China*

¹⁵ *Helmholtz Institute Mainz, Johann-Joachim-Becher-Weg 45, D-55099 Mainz, Germany*

¹⁶ *Henan Normal University, Xinxiang 453007, People's Republic of China*

¹⁷ *Henan University of Science and Technology, Luoyang 471003, People's Republic of China*

¹⁸ *Huangshan College, Huangshan 245000, People's Republic of China*

¹⁹ *Hunan Normal University, Changsha 410081, People's Republic of China*

²⁰ *Hunan University, Changsha 410082, People's Republic of China*

²¹ *Indian Institute of Technology Madras, Chennai 600036, India*

²² *Indiana University, Bloomington, Indiana 47405, USA*

²³ *(A)INFN Laboratori Nazionali di Frascati, I-00044, Frascati, Italy; (B)INFN and University of Perugia, I-06100, Perugia, Italy*

²⁴ *(A)INFN Sezione di Ferrara, I-44122, Ferrara,*

Italy; (B)University of Ferrara, I-44122, Ferrara, Italy

²⁵ *Institute of Physics and Technology, Peace Ave. 54B, Ulaanbaatar 13330, Mongolia*

²⁶ *Johannes Gutenberg University of Mainz, Johann-Joachim-Becher-Weg 45, D-55099 Mainz, Germany*

²⁷ *Joint Institute for Nuclear Research, 141980 Dubna, Moscow region, Russia*

²⁸ *Justus-Liebig-Universitaet Giessen, II. Physikalisches Institut, Heinrich-Buff-Ring 16, D-35392 Giessen, Germany*

²⁹ *KVI-CART, University of Groningen, NL-9747 AA Groningen, The Netherlands*

³⁰ *Lanzhou University, Lanzhou 730000, People's Republic of China*

³¹ *Liaoning University, Shenyang 110036, People's Republic of China*

³² *Nanjing Normal University, Nanjing 210023, People's Republic of China*

³³ *Nanjing University, Nanjing 210093, People's Republic of China*

³⁴ *Nankai University, Tianjin 300071, People's Republic of China*

³⁵ *Peking University, Beijing 100871, People's Republic of China*

³⁶ *Shandong University, Jinan 250100, People's Republic of China*

³⁷ *Shanghai Jiao Tong University, Shanghai 200240, People's Republic of China*

³⁸ *Shanxi University, Taiyuan 030006, People's Republic of China*

³⁹ *Sichuan University, Chengdu 610064, People's Republic of China*

⁴⁰ *Soochow University, Suzhou 215006, People's Republic of China*

⁴¹ *Southeast University, Nanjing 211100, People's Republic of China*

⁴² *State Key Laboratory of Particle Detection and Electronics,*

Beijing 100049, Hefei 230026, People's Republic of China

⁴³ *Sun Yat-Sen University, Guangzhou 510275, People's Republic of China*

⁴⁴ *Tsinghua University, Beijing 100084, People's Republic of China*

⁴⁵ *(A)Ankara University, 06100 Tandogan, Ankara,*

Turkey; (B)Istanbul Bilgi University, 34060 Eyup,

Istanbul, Turkey; (C)Uhdag University, 16059 Bursa,

Turkey; (D)Near East University, Nicosia, North Cyprus, Mersin 10, Turkey

⁴⁶ *University of Chinese Academy of Sciences, Beijing 100049, People's Republic of China*

- ⁴⁷ University of Hawaii, Honolulu, Hawaii 96822, USA
⁴⁸ University of Jinan, Jinan 250022, People's Republic of China
⁴⁹ University of Minnesota, Minneapolis, Minnesota 55455, USA
⁵⁰ University of Muenster, Wilhelm-Klemm-Str. 9, 48149 Muenster, Germany
⁵¹ University of Science and Technology Liaoning, Anshan 114051, People's Republic of China
⁵² University of Science and Technology of China, Hefei 230026, People's Republic of China
⁵³ University of South China, Hengyang 421001, People's Republic of China
⁵⁴ University of the Punjab, Lahore-54590, Pakistan
⁵⁵ (A)University of Turin, I-10125, Turin, Italy; (B)University of Eastern Piedmont, I-15121, Alessandria, Italy; (C)INFN, I-10125, Turin, Italy
⁵⁶ Uppsala University, Box 516, SE-75120 Uppsala, Sweden
⁵⁷ Wuhan University, Wuhan 430072, People's Republic of China
⁵⁸ Xinyang Normal University, Xinyang 464000, People's Republic of China
⁵⁹ Zhejiang University, Hangzhou 310027, People's Republic of China
⁶⁰ Zhengzhou University, Zhengzhou 450001, People's Republic of China
- ^a Also at Bogazici University, 34342 Istanbul, Turkey
^b Also at the Moscow Institute of Physics and Technology, Moscow 141700, Russia
^c Also at the Functional Electronics Laboratory, Tomsk State University, Tomsk, 634050, Russia
^d Also at the Novosibirsk State University, Novosibirsk, 630090, Russia
^e Also at the NRC "Kurchatov Institute", PNPI, 188300, Gatchina, Russia
^f Also at Istanbul Arel University, 34295 Istanbul, Turkey
^g Also at Goethe University Frankfurt, 60323 Frankfurt am Main, Germany
^h Also at Key Laboratory for Particle Physics, Astrophysics and Cosmology, Ministry of Education; Shanghai Key Laboratory for Particle Physics and Cosmology; Institute of Nuclear and Particle Physics, Shanghai 200240, People's Republic of China
ⁱ Also at Government College Women University, Sialkot - 51310. Punjab, Pakistan.
^j Also at Key Laboratory of Nuclear Physics and Ion-beam Application (MOE) and Institute of Modern Physics, Fudan University, Shanghai 200443, People's Republic of China
^k Also at Harvard University, Department of Physics, Cambridge, MA, 02138, USA
- (Dated: January 15, 2019)

Using a total of 9.0 fb^{-1} of e^+e^- collision data with center-of-mass energies between 4.15 and 4.30 GeV collected by the BESIII detector, we search for the processes $e^+e^- \rightarrow \gamma X(3872)$ with $X(3872) \rightarrow \pi^0 \chi_{cJ}$ for $J = 0, 1, 2$. We report the first observation of $X(3872) \rightarrow \pi^0 \chi_{c1}$, a new decay mode of the $X(3872)$, with a statistical significance of more than 5σ . Normalizing to the previously established process $e^+e^- \rightarrow \gamma X(3872)$ with $X(3872) \rightarrow \pi^+\pi^- J/\psi$, we find $\mathcal{B}(X(3872) \rightarrow \pi^0 \chi_{c1})/\mathcal{B}(X(3872) \rightarrow \pi^+\pi^- J/\psi) = 0.88_{-0.27}^{+0.33} \pm 0.10$, where the first error is statistical and the second is systematic. We set 90% confidence level upper limits on the corresponding ratios for the decays to $\pi^0 \chi_{c0}$ and $\pi^0 \chi_{c2}$ of 19 and 1.1, respectively.

PACS numbers: 13.25.Gv, 14.40.Pq, 14.40.Rt

In the mass region above open-charm threshold, where charmonium states are heavy enough to decay to open-charm mesons, there are a number of states with features that are yet to be satisfactorily understood [1]. These features likely point towards the existence of non- $c\bar{c}$ configurations of charmonium. The $X(3872)$ (also known as the $\chi_{c1}(3872)$) was the first of these unexpected states to be discovered. It was first observed in 2003 by the Belle Collaboration in the process $B \rightarrow KX(3872)$ with $X(3872) \rightarrow \pi^+\pi^- J/\psi$ [2]. It has since been seen by many other experiments in other processes and decay modes [3]. Its prominent features now include: its width is narrow ($\Gamma < 1.2 \text{ MeV}/c^2$) [4]; its mass is consistent with the $D^0\bar{D}^{*0}$ threshold (with an error on the mass difference of $0.18 \text{ MeV}/c^2$) [3]; it has quantum numbers $J^{PC} = 1^{++}$ [5]; no isospin partners are currently known [6]; it has isospin-violating decays since it decays to both $\rho J/\psi$ [4] and $\omega J/\psi$ [7]; it also decays to $D^0\bar{D}^{*0}$ [8], $\gamma J/\psi$ [9], and $\gamma\psi(2S)$ [9]. Despite

this growing list of experimental facts, the nature of the $X(3872)$ remains unclear [1]. Measuring pionic transitions of the $X(3872)$ to the χ_{cJ} has been proposed to be one way to distinguish between various interpretations. If the $X(3872)$ were a conventional $c\bar{c}$ state, transitions to the χ_{cJ} should be very small (Ref. [10] predicts $\Gamma(X(3872) \rightarrow \pi^0 \chi_{c1}) \sim 0.06 \text{ keV}$); if the $X(3872)$ were a tetraquark or molecular state, on the other hand, these rates are expected to be sizeable [10, 11].

The BESIII experiment, operating at the Beijing Electron Positron Collider (BEPCII), previously observed the process $e^+e^- \rightarrow \gamma X(3872)$ with $X(3872) \rightarrow \pi^+\pi^- J/\psi$ using data collected at four center-of-mass energies (E_{CM}): 4.01, 4.23, 4.26, and 4.36 GeV [12]. The cross section was shown to be largest at 4.23 and 4.26 GeV. Since that time, BESIII has collected more data in this energy region, including approximately 3 fb^{-1} at 4.18 GeV and 0.5 fb^{-1} at each of seven additional points between 4.19 and 4.27 GeV. These additional data sets

provide an opportunity to search for new decay modes of the $X(3872)$ using the same production process $e^+e^- \rightarrow \gamma X(3872)$. Data collected at different E_{CM} can be combined and new $X(3872)$ decays can be normalized to $e^+e^- \rightarrow \gamma X(3872)$ with $X(3872) \rightarrow \pi^+\pi^-J/\psi$, thereby canceling the production cross section and many systematic uncertainties.

In this Letter, we report the first observation of the decay $X(3872) \rightarrow \pi^0\chi_{c1}$ with a statistical significance of 5.2σ . Like the $\rho J/\psi$ decay, this final state has an isospin of one. This is the first observation of a decay of the $X(3872)$ to a P -wave charmonium state and its large branching fraction relative to $\pi^+\pi^-J/\psi$ supports a non- $c\bar{c}$ interpretation of the $X(3872)$ [10, 11].

We search for the processes $e^+e^- \rightarrow \gamma_1 X(3872)$ with $X(3872) \rightarrow \pi^0\chi_{cJ}$ ($J = 0, 1, 2$) using the decays $\chi_{cJ} \rightarrow \gamma_2 J/\psi$ and $J/\psi \rightarrow l^+l^-$, where l^+l^- denotes both e^+e^- and $\mu^+\mu^-$, and γ_1 and γ_2 are the initial photon and the photon from the χ_{cJ} decay, respectively. This is subsequently referred to as the “search” channel and it results in the final state $\gamma_1\gamma_2\pi^0l^+l^-$ (with $\pi^0 \rightarrow \gamma\gamma$). We also reconstruct the “normalization” channel $e^+e^- \rightarrow \gamma X(3872)$ with $X(3872) \rightarrow \pi^+\pi^-J/\psi$ and $J/\psi \rightarrow l^+l^-$, resulting in the final state $\gamma\pi^+\pi^-l^+l^-$. For the signal region, we use all available BESIII data with E_{CM} between 4.15 and 4.30 GeV (9.0 fb^{-1}), where the $e^+e^- \rightarrow \gamma X(3872)$ cross section was measured to be largest; and for the sideband regions, we use all data with E_{CM} between 4.00 and 4.15 GeV (0.7 fb^{-1}) and between 4.30 and 4.60 GeV (2.8 fb^{-1}).

The Beijing Spectrometer (BESIII) experiment uses a general purpose magnetic spectrometer [13]. A superconducting solenoid magnet provides a 1.0 T magnetic field. Enclosed within the magnet are a helium-gas-based drift chamber (MDC) for charged particle tracking and a CsI(Tl) Electromagnetic Calorimeter (EMC) to measure the energy of electromagnetic showers. Other detector components, such as the plastic scintillator time-of-flight system (TOF), are not used in this analysis.

A GEANT4-based [14] Monte Carlo (MC) simulation package is used to determine detection efficiencies and estimate background rates. The initial e^+e^- collisions, including effects due to Initial State Radiation (ISR), and subsequent decays are simulated using KKMC [15] and EVTGEN [16], respectively. Final State Radiation (FSR) is simulated with PHOTOS [17].

Optimization of the event selection criteria is performed using three categories of data samples: one to estimate signal yields (S), and two for background yields (B_1 and B_2). For S , signal MC samples are used. The normalization channel is generated so that $\sigma(e^+e^- \rightarrow \gamma X(3872)) \times \mathcal{B}(X(3872) \rightarrow \pi^+\pi^-J/\psi) = 0.3 \text{ pb}$ at each E_{CM} [12]; the search channels are initially scaled assuming $\mathcal{B}(X(3872) \rightarrow \pi^0\chi_{cJ})/\mathcal{B}(X(3872) \rightarrow \pi^+\pi^-J/\psi) = 1$. For B_1 , background MC samples for processes including a J/ψ are generated using previously measured cross sections. These include $e^+e^- \rightarrow \pi\pi J/\psi$ [18, 19], $\pi\pi\psi(3686)$ [20, 21], $\eta J/\psi$ [22], $\eta' J/\psi$ [23],

$\omega\chi_{cJ}$ [24, 25], and $\gamma_{\text{ISR}}\psi(3686)$ [26, 27]. These also include $e^+e^- \rightarrow \gamma X(3872)$ with $X(3872)$ decays to $\omega J/\psi$ [7], $\gamma J/\psi$ [9] and $\gamma\psi(3686)$ [9], each of which is normalized to $X(3872) \rightarrow \pi^+\pi^-J/\psi$ using previous measurements [3]. For B_2 , background modes that do not include a J/ψ are estimated using sidebands in the reconstructed mass spectrum of J/ψ candidates in data. Analysis of an inclusive MC sample shows no other background modes with peaks near the J/ψ , χ_{cJ} , or $X(3872)$ masses.

Common charged particle and photon selection criteria are used for the normalization and search channels. Charged particles are selected using their distance of closest approach to the interaction region (within 10 cm along the beam direction and 1 cm transverse to it) and are required to be within the region $|\cos\theta| < 0.93$, where θ is measured with respect to the beam axis. No particle identification is used for charged pions. Electrons and muons are distinguished using the energy they deposit in the EMC divided by their momentum (E/p): charged tracks are labeled as electrons (muons) in the case $E/p > 0.85$ ($E/p < 0.25$), respectively. Photons must have deposited an energy greater than 25 MeV in the barrel region of the EMC ($|\cos\theta| < 0.80$) and greater than 50 MeV in the endcap region ($0.86 < |\cos\theta| < 0.92$), and must have a hit time within 700 ns of the event start time.

Using the selected charged particles and photons, kinematic fits are then performed for the normalization channel ($\gamma\pi^+\pi^-l^+l^-$) and search channel ($\gamma_1\gamma_2\pi^0l^+l^-$) hypotheses. A four-constraint (4C) kinematic fit is used for the normalization channel, where the total measured four-momentum is constrained to the four-momentum of the initial center-of-mass system, and the resulting χ_{4C}^2/dof is required to be less than 10. For the search channel, an extra constraint (1C) is added to constrain a $\gamma\gamma$ pair to the π^0 mass and we require $\chi_{5C}^2/\text{dof} < 5$. These criteria are optimized by maximizing $S/\sqrt{S+B_1+B_2}$, where the sizes of the signal (S) and background (B_1 and B_2) are determined from the three data samples described previously. Multiple combinations per event are allowed, but are negligible after event selection. Using signal MC samples, multiply counted events are found to be less than 0.1% and 4% in the normalization and search channels, respectively. In data, no multiply counted events are found.

The J/ψ signal is selected by requiring $M(l^+l^-)$ to be within 20 MeV/ c^2 of the nominal J/ψ mass [3]. The J/ψ sideband regions, used for background estimations, are each 40 MeV/ c^2 wide on either side of the J/ψ and leave a 20 MeV/ c^2 gap with the signal region.

Several additional criteria are used to select the normalization channel. Radiative Bhabha background events ($e^+e^- \rightarrow e^+e^-(n\gamma)$), where a radiated photon converts to e^+e^- within the detector material and the resulting e^+e^- are mistaken to be $\pi^+\pi^-$, are removed by requiring the $\pi^+\pi^-$ opening angle ($\theta_{\pi\pi}$) to satisfy $\cos\theta_{\pi\pi} < 0.98$. Further suppression of this background

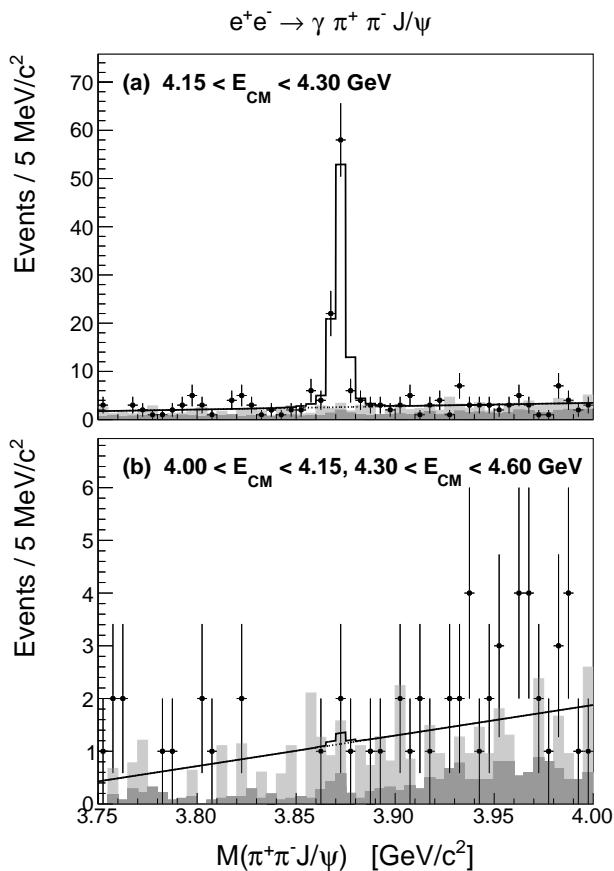


FIG. 1. Distribution of $\pi^+\pi^-J/\psi$ mass, $M(\pi^+\pi^-J/\psi)$, from the normalization process $e^+e^- \rightarrow \gamma\pi^+\pi^-J/\psi$ for (a) $4.15 < E_{\text{CM}} < 4.30$ GeV and (b) $4.00 < E_{\text{CM}} < 4.15$ or $4.30 < E_{\text{CM}} < 4.60$ GeV. Points are data; lines are fits (solid is the total and dotted is the polynomial background); the darker histogram is a MC estimate of peaking J/ψ backgrounds; the lighter stacked histogram is an estimate of non-peaking backgrounds using J/ψ sidebands from data.

process is obtained by requiring the opening angle of the final-state photon and any charged track ($\theta_{\gamma\text{tk}}$) to satisfy $\cos\theta_{\gamma\text{tk}} < 0.98$. Background events from $\eta J/\psi$ and $\eta' J/\psi$ are removed by requiring $M(\gamma\pi^+\pi^-) > 0.6$ GeV/ c^2 and $|M(\gamma\pi^+\pi^-) - M_0(\eta')| > 0.02$ GeV/ c^2 ($M_0(\eta')$ is the nominal mass of the η' [3]), respectively.

For the search channel, the background mode $\pi^0\pi^0 J/\psi$ is suppressed both by requiring $M(\gamma_1\gamma_2)$ to be 20 MeV/ c^2 away from the π^0 mass and by placing the same requirement on the mass of γ_1 or γ_2 combined with the higher energy photon from the π^0 decay. Background events from $\omega(782)$ decays to $\gamma\pi^0$, including those from $e^+e^- \rightarrow \omega\chi_{cJ}$ and $\gamma X(3872) \rightarrow \gamma\omega J/\psi$, are removed by requiring $M(\gamma_{1,2}\pi^0) < 0.732$ GeV/ c^2 . Finally, background events from $\gamma_{\text{ISR}}\psi(3686)$ are reduced by requiring the mass recoiling against γ_1 or γ_2 both to be larger than 3.7 GeV/ c^2 .

The final distributions for the reconstructed $\pi^+\pi^-J/\psi$ mass in the normalization channel are shown in Fig. 1.

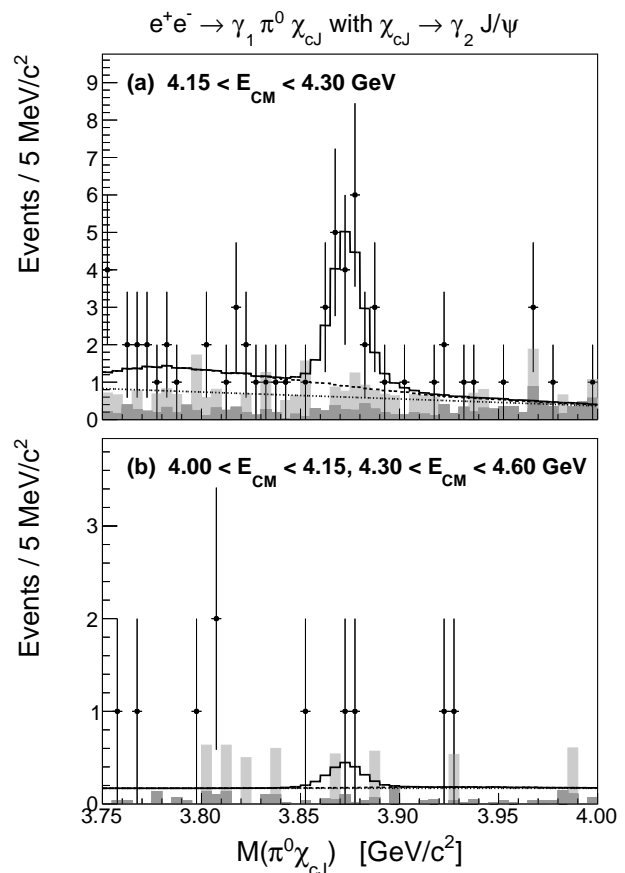


FIG. 2. Distribution of $\pi^0\chi_{cJ}$ mass, $M(\pi^0\chi_{cJ})$, from the process $e^+e^- \rightarrow \gamma\pi^0\chi_{cJ}$ for (a) $4.15 < E_{\text{CM}} < 4.30$ GeV and (b) $4.00 < E_{\text{CM}} < 4.15$ or $4.30 < E_{\text{CM}} < 4.60$ GeV. The χ_{cJ} are selected using a broad region of $\gamma J/\psi$ mass. Points, lines, and histograms follow the same convention as Fig. 1. The dashed line is the total background contribution to the fit, including signal events with γ_1 and γ_2 interchanged.

In order to improve the mass resolution, $M(\pi^+\pi^-J/\psi)$ is calculated using $M(\pi^+\pi^-l^+l^-) - M(l^+l^-) + M_0(J/\psi)$, where $M_0(J/\psi)$ is the nominal mass of the J/ψ . The mass resolution is improved from 7.4 MeV/ c^2 to 4.7 MeV/ c^2 . Figure 1a corresponds to data taken at $4.15 < E_{\text{CM}} < 4.30$ GeV and shows a clear $X(3872)$ signal. The data are fitted by a first-order polynomial representing the background and a response function of the signal process that has been obtained from the signal MC simulation. All fits are performed using a binned likelihood method; all significances are obtained by comparing the resulting likelihoods with and without the signal component included. Results are listed in Table I. Figure 1b shows the same for the other E_{CM} samples. No $X(3872)$ signal is seen. This pattern is consistent with the previous measurement [12].

The corresponding distributions of $M(\pi^0\chi_{cJ})$ for the search channel are shown in Fig. 2. The χ_{cJ} region is first chosen with a loose requirement on $M(\gamma_{1,2}J/\psi) \equiv M(\gamma_{1,2}l^+l^-) - M(l^+l^-) + M_0(J/\psi)$ between 3.35 and

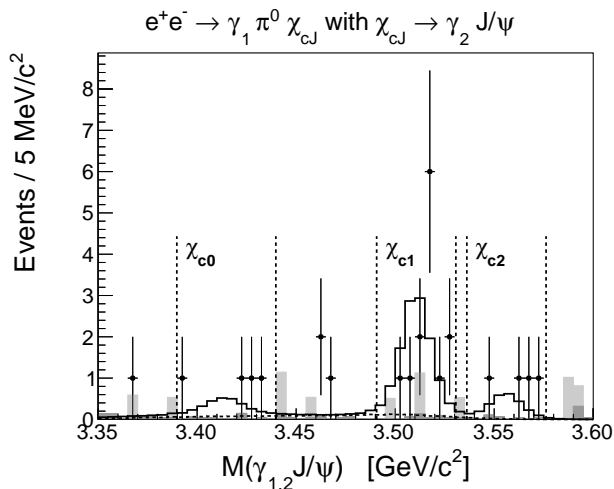


FIG. 3. Distribution of $M(\gamma_{1,2}J/\psi)$ after selecting the $X(3872)$ signal region from Fig. 2a. Points and shaded histograms follow the same convention as Fig. 1. The solid line is the signal MC and is scaled using subsequent fits; the dashed line is the component of the signal MC where γ_1 and γ_2 are interchanged. Vertical lines show the χ_{cJ} selection regions.

$3.60 \text{ GeV}/c^2$. A clear signal for the $X(3872)$ is observed for $4.15 < E_{CM} < 4.30 \text{ GeV}$ (Fig. 2a); no evidence for the $X(3872)$ is seen at other E_{CM} (Fig. 2b). The distributions are fit with a first-order polynomial background function and a signal shape derived from the signal MC simulation, where the relative fractions of $\pi^0\chi_{cJ}$ with $J = 0, 1, 2$ are fixed by subsequent fits. There are two entries per event corresponding to the two combinations of γ_1 and γ_2 ; the signal MC includes a broad contribution from events with interchanged γ_1 and γ_2 . Using the background samples described earlier (B_1 and B_2), we find no other peaking background events. The fit in Fig. 2a yields $16.9^{+5.2}_{-4.5}$ $X(3872)$ events with a statistical significance of 4.8σ .

We next use the $M(\gamma_{1,2}J/\psi)$ distribution to select the χ_{c0} , χ_{c1} , and χ_{c2} mass regions (Fig. 3). The photons γ_1 and γ_2 are separated by choosing γ_2 to be the photon that minimizes $\Delta M_J \equiv |M(\gamma_2 J/\psi) - M_0(\chi_{cJ})|$, where $M_0(\chi_{cJ})$ is the nominal mass of each χ_{cJ} [3]. We require $\Delta M_0 < 25 \text{ MeV}/c^2$ and $\Delta M_{1,2} < 20 \text{ MeV}/c^2$. The resulting distributions for $M(\pi^0\chi_{cJ})$ with $J = 0, 1, 2$ are shown in Fig. 4. Each $M(\pi^0\chi_{cJ})$ distribution is fit with a constant background function and a signal shape derived from signal MC simulation. The signal MC samples include events with interchanged γ_1 and γ_2 as well as cross-feed among the $\pi^0\chi_{cJ}$ channels. These effects result in an additional peak below the $X(3872)$ signal region in the $M(\pi^0\chi_{c0})$ distribution, but are negligible elsewhere. In the $M(\pi^0\chi_{c1})$ distribution, we find a $X(3872)$ signal with a 5.2σ significance. No significant $X(3872)$ signals are found in the $M(\pi^0\chi_{c0,2})$ distributions. Numbers for events, efficiencies, and significances are listed in Table I. The total yield of signal events in all three channels is $15.1^{+4.8}_{-3.8}$, consistent with the fit in Fig. 2a.

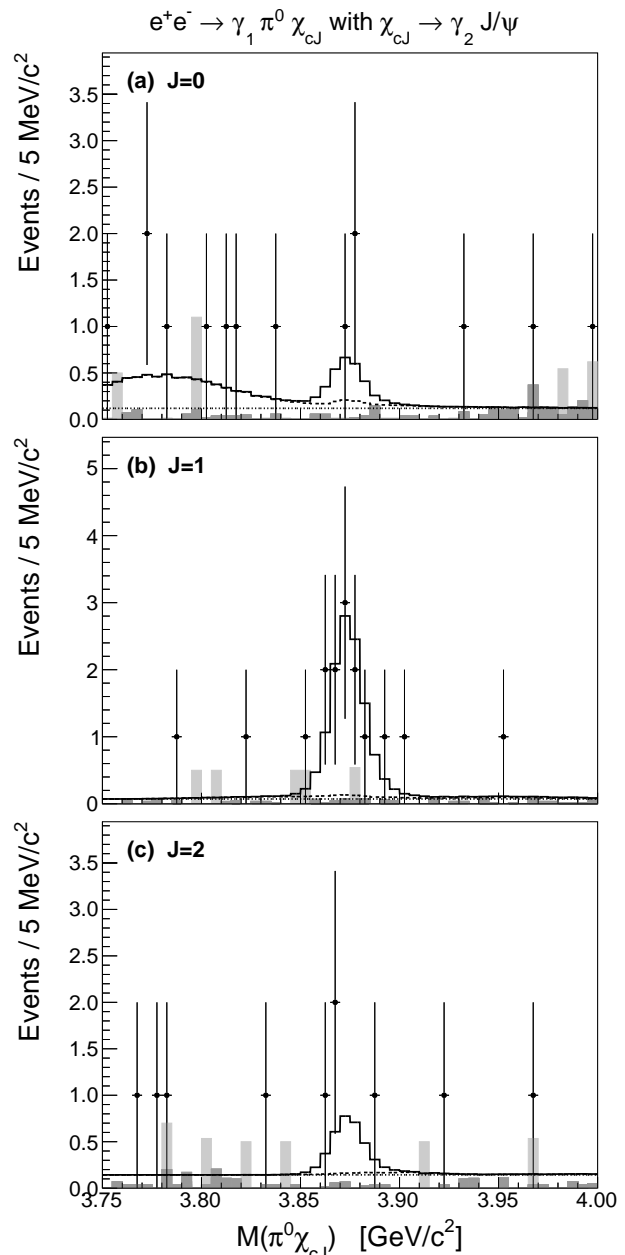


FIG. 4. Distributions of $\pi^0\chi_{cJ}$ mass, $M(\pi^0\chi_{cJ})$, from the process $e^+e^- \rightarrow \gamma\pi^0\chi_{cJ}$ for (a) $J = 0$, (b) $J = 1$, and (c) $J = 2$. Points, lines, and histograms follow the same convention as Fig. 1. The dashed line is the total background in the fit and includes contributions from events with interchanged γ_1 and γ_2 and cross-feed among the search channels.

Also shown in Table I are the final ratios $\mathcal{B}(X(3872) \rightarrow \pi^0\chi_{cJ})/\mathcal{B}(X(3872) \rightarrow \pi^+\pi^-J/\psi)$. These are calculated from the ratios of yields of signal events, the ratios of efficiencies (including minor effects due to ISR), and the nominal χ_{cJ} and π^0 branching fractions [3]. Upper limits (at the 90% C.L.) are calculated from the likelihood curve of the fits as a function of signal yield after being convolved with a Gaussian distribution with a width the size of the systematic uncertainty. The J/ψ branch-

ing fractions, integrated luminosities at each E_{CM} , ISR correction factors, as well as a number of systematic uncertainties cancel in the ratios.

The remaining systematic uncertainties are listed in Table II. (1,2) For uncertainties in the photon and charged track efficiencies, we use 1% per photon [28] and track [23] that do not cancel between the search and normalization channels. (3) For input branching fractions, uncertainties from the PDG are used [3]. (4) A systematic uncertainty due to the kinematic fit is determined using clean control samples with matching final states: $e^+e^- \rightarrow \pi^0\pi^0 J/\psi$ for the search channel and $e^+e^- \rightarrow \gamma_{\text{ISR}}\psi(2S) \rightarrow \gamma_{\text{ISR}}\pi^+\pi^- J/\psi$ for the normalization channel. (5) The selection criteria that distinguish between γ_1 and γ_2 in the search channel introduce some E_{CM} -dependence in the efficiency ratio. To probe this uncertainty, we generate different shapes for the cross section as a function of E_{CM} : the nominal is constant, one is based on the $e^+e^- \rightarrow \pi^+\pi^- J/\psi$ lineshape seen by BESIII [18], and one is based on the $\psi(4160)$ lineshape with parameters from the PDG [3]. We take the largest difference as a systematic uncertainty. (6) Signal MC samples are generated according to realistic spin-dependent amplitudes using EVTGEN [16]. In channels where there is ambiguity (e.g. the presence of both S - and D -waves in $X(3872) \rightarrow \rho J/\psi$ [4] or both P - and F -waves in $X(3872) \rightarrow \pi^0\chi_{c2}$), we replace our nominal models by phase space and take the maximum difference as a systematic uncertainty. (7) Fitting uncertainties are evaluated using two fit variations: zeroth- and first-order background polynomials, and a signal shape that is widened by 20% to account for possible differences in mass resolution between data and MC simulation. The significance of the signal for $X(3872) \rightarrow \pi^0\chi_{c1}$ remains above 5σ for all variations. The total systematic uncertainty is obtained by adding the individual uncertainties in quadrature.

In summary, we use 9.0 fb^{-1} of e^+e^- collision data with E_{CM} between 4.15 and 4.30 GeV to search for the processes $e^+e^- \rightarrow \gamma X(3872)$ with $X(3872) \rightarrow \pi^0\chi_{cJ}$. We make the first observation of the process $X(3872) \rightarrow \pi^0\chi_{c1}$, where the statistical significance is greater than 5σ for all systematic variations. Normalizing to $e^+e^- \rightarrow \gamma X(3872)$ with $X(3872) \rightarrow \pi^+\pi^- J/\psi$, we determine the ratio $\mathcal{B}(X(3872) \rightarrow \pi^0\chi_{c1})/\mathcal{B}(X(3872) \rightarrow$

$\pi^+\pi^- J/\psi) = 0.88_{-0.27}^{+0.33} \pm 0.10$. Upper limits (at the 90% C.L.) for the corresponding ratios for the $\pi^0\chi_{c0}$ and $\pi^0\chi_{c2}$ decays are 19 and 1.1, respectively. Using $\mathcal{B}(X(3872) \rightarrow \pi^+\pi^- J/\psi) > 3.2\%$ [3] (obtained by comparing exclusive [29] and inclusive [30] B^+ decays) and $\mathcal{B}(X(3872) \rightarrow \pi^+\pi^- J/\psi) < 6.4\%$ (obtained by assuming all measured $X(3872)$ decays add to less than 100%), we find $\mathcal{B}(X(3872) \rightarrow \pi^0\chi_{c1}) \sim 3 - 6\%$. If the $X(3872)$ were the $\chi_{c1}(2P)$ state of charmonium, Ref. [10] predicts $\Gamma(X(3872) \rightarrow \pi^0\chi_{c1}) \sim 0.06 \text{ keV}$. Combining this with our result, this would imply a total width of the $X(3872)$ of only $\sim 1.0 - 2.0 \text{ keV}$, which would be orders of magnitude smaller than all other observed charmonium states. Therefore, our measurement disfavors the $c\bar{c}$ interpretation of the $X(3872)$.

The BESIII collaboration thanks the staff of BEPCII and the IHEP computing center for their strong support. This work is supported in part by National Key Basic Research Program of China under Contract No. 2015CB856700; National Natural Science Foundation of China (NSFC) under Contracts Nos. 11335008, 11425524, 11625523, 11635010, 11735014; the Chinese Academy of Sciences (CAS) Large-Scale Scientific Facility Program; the CAS Center for Excellence in Particle Physics (CCEPP); Joint Large-Scale Scientific Facility Funds of the NSFC and CAS under Contracts Nos. U1532257, U1532258, U1732263; CAS Key Research Program of Frontier Sciences under Contracts Nos. QYZDJ-SSW-SLH003, QYZDJ-SSW-SLH040; 100 Talents Program of CAS; INPAC and Shanghai Key Laboratory for Particle Physics and Cosmology; German Research Foundation DFG under Contract No. Collaborative Research Center CRC 1044; Istituto Nazionale di Fisica Nucleare, Italy; Koninklijke Nederlandse Akademie van Wetenschappen (KNAW) under Contract No. 530-4CDP03; Ministry of Development of Turkey under Contract No. DPT2006K-120470; National Science and Technology fund; The Swedish Research Council; the Knut and Alice Wallenberg foundation; U. S. Department of Energy under Contracts Nos. DE-FG02-05ER41374, DE-SC-0010118, DE-SC-0012069; University of Groningen (RuG) and the Helmholtzzentrum fuer Schwerionenforschung GmbH (GSI), Darmstadt.

[1] R. F. Lebed, R. E. Mitchell and E. S. Swanson, Prog. Part. Nucl. Phys. **93**, 143 (2017); H. X. Chen, W. Chen, X. Liu and S. L. Zhu, Phys. Rept. **639**, 1 (2016); A. Esposito, A. Pilloni and A. D. Polosa, Phys. Rept. **668**, 1 (2016); F. K. Guo, C. Hanhart, U. G. Meißner, Q. Wang, Q. Zhao and B. S. Zou, Rev. Mod. Phys. **90**, 015004 (2018); A. Ali, J. S. Lange and S. Stone, Prog. Part. Nucl. Phys. **97**, 123 (2017); S. L. Olsen, T. Skwarnicki and D. Zieminska, Rev. Mod. Phys. **90**, 015003 (2018).
 [2] S.-K. Choi *et al.* (Belle Collaboration), Phys. Rev. Lett.

91, 262001 (2003).
 [3] C. Patrignani *et al.* (Particle Data Group), Chin. Phys. C **40**, 100001 (2016).
 [4] S.-K. Choi *et al.*, Phys. Rev. D **84**, 052004 (2011).
 [5] R. Aaij *et al.* (LHCb Collaboration), Phys. Rev. D **92**, 011102 (2015).
 [6] B. Aubert *et al.* (BaBar Collaboration), Phys. Rev. D **71**, 031501 (2005).
 [7] P. del Amo Sanchez *et al.* (BaBar Collaboration), Phys. Rev. D **82**, 011101 (2010).

TABLE I. Final results for the normalization and search channels and their ratios. Individual efficiencies are reported without considering ISR in the MC (no ISR) and are for illustration only. Efficiency ratios are for the search channels divided by the normalization channel and include effects due to ISR (with ISR), which nearly cancel in the ratio. Numbers in parentheses are 90% C.L. upper limits. The first errors are statistical and the second are systematic.

	$\pi^+\pi^-J/\psi$	$\pi^0\chi_{c0}$	$\pi^0\chi_{c1}$	$\pi^0\chi_{c2}$
Event yield	$84.1^{+10.1}_{-9.4}$	$1.9^{+1.9}_{-1.3}$	$10.8^{+3.8}_{-3.1}$	$2.5^{+2.3}_{-1.7}$
Signal significance (σ)	16.1	1.6	5.2	1.6
Efficiency (no ISR) (%)	32.3	8.8	14.1	12.8
Efficiency ratio (with ISR)	...	0.272	0.435	0.392
$\mathcal{B}(\chi_{cJ} \rightarrow \gamma J/\psi) \times \mathcal{B}(\pi^0 \rightarrow \gamma\gamma)$ (%)	...	1.3	33.5	19.0
Total systematic error (%)	...	17.0	11.9	9.4
$\mathcal{B}(X \rightarrow \pi^0\chi_{cJ})/\mathcal{B}(X \rightarrow \pi^+\pi^-J/\psi)$...	$6.6^{+6.5}_{-4.5} \pm 1.1$ (19)	$0.88^{+0.33}_{-0.27} \pm 0.10$	$0.40^{+0.37}_{-0.27} \pm 0.04$ (1.1)

TABLE II. Relative systematic uncertainties on the ratio $\mathcal{B}(X(3872) \rightarrow \pi^0\chi_{cJ})/\mathcal{B}(X(3872) \rightarrow \pi^+\pi^-J/\psi)$ for $J = 0, 1, 2$. All entries are in percent.

	$\pi^0\chi_{c0}$	$\pi^0\chi_{c1}$	$\pi^0\chi_{c2}$
(1) Photon efficiencies	3.0	3.0	3.0
(2) Track efficiencies	2.0	2.0	2.0
(3) Input branching fractions	4.7	3.5	3.6
(4) Kinematic fit	4.6	4.6	4.6
(5) E_{CM} -dependence of efficiency ratio	3.2	5.2	5.2
(6) MC decay models	8.2	8.1	2.3
(7) Fitting to determine signal yield	12.4	1.6	3.0
Total	17.0	11.9	9.4

[8] G. Gokhroo *et al.* (Belle Collaboration), Phys. Rev. Lett. **97**, 162002 (2006).
[9] R. Aaij *et al.* (LHCb Collaboration), Nucl. Phys. B **886**, 665 (2014).
[10] S. Dubynskiy and M. B. Voloshin, Phys. Rev. D **77**, 014013 (2008).
[11] S. Fleming and T. Mehen, Phys. Rev. D **78**, 094019 (2008); T. Mehen, Phys. Rev. D **92**, 034019 (2015).
[12] M. Ablikim *et al.* (BESIII Collaboration), Phys. Rev. Lett. **112**, 092001 (2014).
[13] M. Ablikim *et al.* (BESIII Collaboration), Nucl. Instrum. Methods Phys. Res., Sect. A **614**, 345 (2010).
[14] S. Agostinelli *et al.* (GEANT4 Collaboration), Nucl. Instrum. Methods Phys. Res., Sect. A **506**, 250 (2003).

[15] S. Jadach, B. F. L. Ward and Z. Was, Phys. Rev. D **63**, 113009 (2001).
[16] D. J. Lange, Nucl. Instrum. Methods Phys. Res., Sect. A **462**, 152 (2001).
[17] P. Golonka and Z. Was, Eur. Phys. J. C **45**, 97 (2006).
[18] M. Ablikim *et al.* (BESIII Collaboration), Phys. Rev. Lett. **118**, 092001 (2017).
[19] M. Ablikim *et al.* (BESIII Collaboration), Phys. Rev. Lett. **115**, 112003 (2015).
[20] M. Ablikim *et al.* (BESIII Collaboration), Phys. Rev. D **96**, 032004 (2017).
[21] M. Ablikim *et al.* (BESIII Collaboration), Phys. Rev. D **97**, 052001 (2018).
[22] M. Ablikim *et al.* (BESIII Collaboration), Phys. Rev. D **91**, 112005 (2015).
[23] M. Ablikim *et al.* (BESIII Collaboration), Phys. Rev. D **94**, 032009 (2016).
[24] M. Ablikim *et al.* (BESIII Collaboration), Phys. Rev. Lett. **114**, 092003 (2015).
[25] M. Ablikim *et al.* (BESIII Collaboration), Phys. Rev. D **93**, 011102 (2016).
[26] E. A. Kuraev and V. S. Fadin, Sov. J. Nucl. Phys. **41**, 466 (1985) [Yad. Fiz. **41**, 733 (1985)].
[27] M. Ablikim *et al.* (BESIII Collaboration), Phys. Lett. B **749**, 414 (2015).
[28] M. Ablikim *et al.* (BESIII Collaboration), Phys. Rev. D **81**, 052005 (2010).
[29] B. Aubert *et al.* (BaBar Collaboration), Phys. Rev. D **77**, 111101 (2008).
[30] Y. Kato *et al.* (Belle Collaboration), Phys. Rev. D **97**, 012005 (2018).